İstanbul Journal of Pharmacy
Istanbul J Pharm2024, 54 (3): 386–394
DOI: 10.26650/IstanbulJPharm.2024.1500047

Original Article

High Performance Liquid Chromatography-Tandem Mass Spectrometric determination of carcinogen nitrosamine impurities from pharmaceuticals and DNA binding confirmation aided by molecular docking application

İbrahim Daniş[1], Soykan Agar[2], Mine Yurtsever[3], Durişehvar Özer Ünal[4]

[1]İstanbul University, Institute of Health Science, Faculty of Pharmacy, Department of Analytical Chemistry; Drug Research Center, İstanbul, Türkiye
[2]Kocaeli Health and Technology University, Faculty of Pharmacy, Department of Biochemistry, In Silico Drug Design Center, Kocaeli, Türkiye
[3]İstanbul Technical University, Department of Chemistry, İstanbul, Türkiye
[4]İstanbul University, Faculty of Pharmacy, Department of Analytical Chemistry; Drug Research Center, İstanbul, Türkiye

ABSTRACT

Background and Aims: Nitrosamines are amine compounds attached to a nitroso group. The reaction of amines and nitrosating agents forms nitrosamines. Nitrosamine impurities are classified as Class 1 based on the carcinogenicity and mutagenicity data by ICH M7 (R1). The recent discovery of nitrosamines in some pharmaceutical products has caused concern. Nitrosamines are carcinogenic, so it is necessary to determine the possible nitrosamines in pharmaceutical products.

Methods: An Inertsil ODS-3, (4.6x250 mm, 5 µm) column was used for separation. A triple quadrupole mass detector with electrospray Ionisation (ESI) was used for detection. Multiple reaction monitoring (MRM) was used for quantification. The transition ions are 75.1 > 43.3 for NDMA and 103.0 > 75.1 for NDEA. The calibration curves consist of 5 concentration levels, including NDMA and NDEA (5, 10, 50, 100, 150 ng/mL). The mean r^2 value was 0.997 for NDMA and 0.999 for NDEA. For NDMA and NDEA, LOD: 2 ng/mL, LOQ: 5 ng/mL.

Results: Comprehensive in silico and in vitro results indicate that the method has good accuracy and precision.

Conclusion: DNA binding interactions of the molecules NDMA and NDEA, were investigated through the molecular docking and molecular dynamics methods. Molecular Docking simulations showed that these small organic molecules have high-affinity scores and strongly bind to the minor groove of the hDNA via strong hydrogen bonds.

Keywords: DNA binding, Molecular docking, MD, Mass spectrometry, Nitrosamine, NDMA, NDEA

INTRODUCTION

Nitrosamines are amine compounds attached to a nitroso group (R1N(-R2)-N=O). Nitrosamines are formed by the reaction of amines and nitrosating agents under acidic conditions (Figure 1). Nitrosamines are amine derivatives that are generally volatile and chemically stable (Control of nitrosamine impurities in human drugs, 2021).

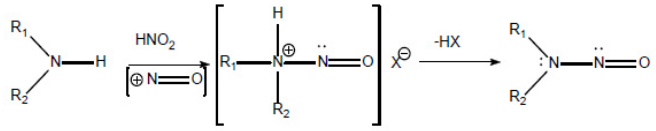

Figure 1. The nitrosamine formation reaction

N-nitroso compounds, which began to be used as solvents in the industry in the 1930s, were later observed to have hepatotoxic effects. Then, due to studies on experimental animals, it was understood that these compounds were not only hepatotoxic but also potent carcinogens (Barnes & Magee, 1954; Magee & Barnes, 1956). In the 1960s, after it was reported that NDMA (N-nitrosodimethylamine) was formed in meat that used nitrite as a preservative, research was started on environmental samples. (Nawrocki & Andrzejewski, 2011; Preussmann, 1984).

The unexpected detection of nitrosamine impurities has highlighted the need to determine their presence in any pharmaceuticals (such as metformin, ranitidine, etc.). In July 2018, the FDA (Food and Drug Administration) and EMA (European Medicines Agency) announced that NDMA and NDEA (N-Nitrosodiethylamine) are found in the drugs, known as "sar-

Corresponding Author: İbrahim Daniş **E-mail:** ibrahimdanis@istanbul.edu.tr
Submitted: 13.06.2024 • **Revision Requested:** 21.08.2024 • **Last Revision Received:** 29.08.2024 • **Accepted:** 16.10.2024

tans", used to treat patients with hypertension. In September 2019, Unacceptable levels of NDMA were found in some common heartburn products (ranitidine, commonly known as Zantac, and nizatidine, commonly known as Axid). In December 2019, some countries reported the presence of NDMA in metformin, which is used for treating type 2 diabetes. In May 2020, tests proved that certain metformin lots contained NDMA above the acceptable intake limit. The FDA and EMA evaluated the processes used in API synthesis and found that common manufacturing processes can reveal other nitrosamine impurities besides NDMA (Nitrosamine impurities in human medicinal products, 2020).

Nitrosamine impurities are classified as Class 1 based on carcinogenicity and mutagenicity data by ICH M7 (R1) (M7(R1) assessment and control of DNA reactive (mutagenic) impurities in pharmaceuticals to limit potential carcinogenic risk, 2018). Nitrosamines are classified as probable human carcinogens by the IARC (International Agency for Research on Cancer) (Ponting, Dobo, Kenyon, & Kalgutkar, 2022). These Nitrosamine impurities affect the genetic material through the DNA adduct. Since the damage caused to DNA by low numbers of nitrosamines threatens human health, it is necessary to determine very low numbers of possible nitrosamines in drug products.

Nitrosamine impurities can be incorporated into drug products mainly through processing, direct administration, cross-contamination, or degradation. The manufacture of drug products includes raw materials, intermediates, reagents, chemicals, and solvents. During these stages, if these impurities are formed, they can be incorporated into the drug products. Secondary, tertiary, and quaternary amines and nitrosating agents such as sodium nitrite are considered to be precursors for the formation of nitrosamine impurities. Recovered solvents and catalysts can pose a risk of nitrosamine formation. These solvents or catalysts can cause the formation of nitrosamine impurities as they are treated with sodium nitrite or nitric acid to remove the residual azide. Contaminated starting material or raw material supplied by the vendor may introduce nitrosamine impurities into the drug product. Cross-contamination in production processes can lead to contamination of nitrosamine impurities. The use of certain packaging materials for the finished product may form nitrosamine impurities. According to one hypothesis, a packaging material containing nitrocellulose can react with amines in the printing ink to form nitrosamine impurities in the drug product. Trace numbers of these impurities may form due to the degradation of the solvents or other materials used in the synthesis of drug substances. Similarly, by-products formed in the drug synthesis process can be transferred to drug substances as nitrosamine impurities. Solvents such as dimethylformamide, dimethylacetamide, or diethylacetamide can form NDMA and NDEA impurities. Experts suggest that the NDMA impurity in valsartan may have come from sodium nitrite, which is used to remove the residual sodium azide (NaN_3) reagent. Under acidic conditions, the nitrite ion forms nitrous acid, which can then react with traces of dimethylamine, a degradation product of the dimethylformamide (DMF) solvent, to form nitrosamine (Figure 2) (Sedlo, Kolonić, & Tomić, 2021; Shaikh, Gosar, & Sayyed, 2020).

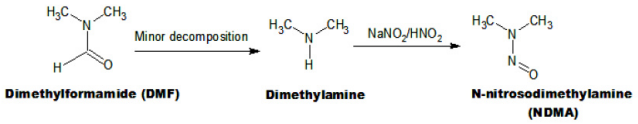

Figure 2. Formation of N-nitrosodimethylamine

The FDA calculated the limit for NDMA and NDEA impurities as 96.0 ng/day and 26.5 ng/day, respectively (Control of nitrosamine impurities in human drugs, 2021).

Some HPLC methods have been reported for nitrosamine impurities. The determination of nitrosamines in food products using the HPLC-UV method with liquid-phase extraction was reported (Li et al., 2018). The determination of nitrosamine in meat using the HPLC method was reported (Al-Kaseem, Al-Assaf, & Karabeet, 2014). An C18 (4.6 × 150 mm, 5 µm) column was used for chromatographic separation. The compounds were detected at a 231 nm wavelength using a spectrophotometric detector. Masada et al. determined the LOD and LOQ for NDMA in valsartan as 8.5 ng/mL and 28.5 ng/mL, respectively (Masada et al., 2019).

Some LC-MS/MS methods have been reported for nitrosamine impurities. The characterisation of nitrosamines in water using the LC-MS/MS method was reported by Zhao et al. (Zhao, Boyd, Hrudey, & Li, 2006). The detection limits were 0.1-10.6 ng/L. Ngongang et al. (Ngongang, Duy, & Sauvé, 2015) reported that nitrosamines can be analysed using LC-MS on a Q-Exactive instrument. The detection limits ranged from 0.4 to 12 ng/L. Scherf-Clavel et al. (Scherf-Clavel et al., 2019) quantified trace amounts of NDMA and NDEA impurities in valsartan samples using the LC-MS method. NDMA was formed during the chlorination of ranitidine as reported by Roux et al. (Roux, Gallard, Croué, Papot, & Deborde, 2012). The detection limit for NDMA formation by ozonation of ranitidine was reported at 4 ng/mL by Lv et al. (Lv, Wang, & Li, 2017).

Atmospheric Pressure Chemical Ionisation (APCI) is a popular complementary soft ionisation technique to Electrospray Ionisation (ESI). LC-MS/MS studies of nitrosamines in the literature have mostly used the APCI ion source. This choice is primarily due to its ability to reduce noise in complex and varied matrices, minimise matrix effects, and analyse very low concentrations. However, the APCI ion source is not as widely used as the ESI ion source, which is more common in LC-MS/MS. In this study, low detection limits were achieved using the ESI ion source. However, by eliminating matrix effects through sam-

ple preparation techniques, the ESI source can also be used efficiently (Kul & Sagirli, 2023).

The molecular docking approach can be used to model the interaction between a small molecule and DNA and a protein at the atomic level, which allows us to characterise the behaviour of small molecules in the binding site of the target (McConkey, Sobolev, & Edelman, 2002). Essentially, molecular docking aims to predict the ligand-receptor complex structure using computation methods. Genotoxicity and carcinogenicity data on nitrosamines are sparse (Thresher et al., 2020). It is thought that some DNAs will guide nitrosamine interaction studies (Li & Hecht, 2022).

The developed and validated method offers an accurate and reliable method for pharmaceutical products, with a calibration curve prepared only by the pre-extraction method and placebo.

MATERIALS AND METHODS

Chemicals and solutions

NDMA and NDEA were purchased from a commercial vendor (Sigma-Aldrich, Germany) and were used as the standard. Acetonitrile and formic acid were purchased from a commercial vendor (Merck KGaA, Darmstadt, Germany) and were used as the solvent and the mobile phase. Deionised water was obtained from a Milli-Q ultrapure water system (Millipore, Barnstead). All reagents and solvents used were of the best analytical grades available.

Chromatographic conditions

The Agilent Technologies liquid chromatography system and 6460 Triple Quad detector system were used in this study. A Inertsil ODS-3, (4.6x250mm, 5µm) column maintained at 40°C was used for separation. The Liquid chromatography mobile phase consisted of acetonitrile:1% formic acid in deionised water (70:30% v/v). The flow rate was 0.600 mL/min. The injection volume was 25.0 µL and the runtime was 10.0 min.

Mass spectrometry conditions

A triple quadrupole mass detector with electrospray Ionisation (ESI) was used for detection. Multiple reaction monitoring (MRM) was used for quantification. The transition ions were 75.1 > 43.3 for NDMA and 103.0 > 75.1 for NDEA, with a dwell time of 100 ms. Nitrogen gas was used as the collision gas. The optimised conditions were 45 psi for nebuliser pressure, 350°C for the gas temperature, 5 L/min for the gas flow, and 3500 V for the capillary. The fragment voltages were 35 V for NDMA and 52 V for NDEA. The collision energies were 14 V for NDMA and 6 V for NDEA.

Preparation of the stock and working solutions

The certified standards were 5 mg/mL for NDMA and 950 mg/mL for NDEA. Intermediate stock solutions for NDMA and NDEA were prepared by diluting the certified standards with acetonitrile. The calibration curve consists of 5 calibration standards. Quality control (QC) samples consist of 3 standards. Calibration standards and QC samples containing both analytes were prepared by diluting the intermediate stock solutions of NDMA and NDEA with acetonitrile to obtain the following analyte concentrations. 5, 10, 50, 100, and 150 ng/mL were prepared for the calibration standards and 5, 75, and 150 ng/mL for the QC samples.

Method validation

The method was validated according to ICH Q2 (R1) on method validation (Guideline, 2005). The evaluated parameters were system suitability, specificity, carryover, accuracy, precision, linearity, LOD, and LOQ.

System suitability

System suitability tests are required for the analytical methods. The overall purpose of system suitability testing is to monitor chromatographic results to ensure chromatographic compatibility and stable system performance. System suitability tests are specific tests that contribute to analytical methods that give accurate and precise results. The system suitability acceptance limits are given according to the FDA guidelines.

Samples preparation

Effervescent, capsule, and tablet drug products were prepared by extracting with acetonitrile. A calibration curve was prepared for each drug product by adding standard impurities to its placebo. After the vortex and centrifugation processes, the samples were filtered into vials and analysed using the validated method.

Matrix Effect

The matrix effect used in the mass spectrometric analysis should be examined. The matrix may increase or decrease the ion intensity, which must be determined. The matrix effect was calculated from the peak areas of the LOQ prepared in the solvent and the LOQ prepared in the relevant sample placebo. The calculated matrix effect is absent when ME = 0%. Ion suppression occurs when ME > 0%, and ion intensity increases when ME < 0%.

Geometry Optimization of the Ligands

Before the simulation studies, the geometries of the ligands, NDMA and NDEA, were optimized using the Gaussian 09 programme (Frisch et al., 2009) with density functional theory (DFT)/B3LYP functional (Becke, 1993) and utilising the 6-31G(d,p) basis set. This process led to the formation of the most stable molecular structures of NDMA and NDEA with 1BNA, intended for further computational and simulation-based research, as depicted in Figures 3 and 4. For molecular docking and molecular dynamics computations, as well as post-processing of the output files, Gauss View 6.0 and Avogadro 1.95 software programmes (Dennington, Keith, & Millam, 2009) were employed to prepare the input files.

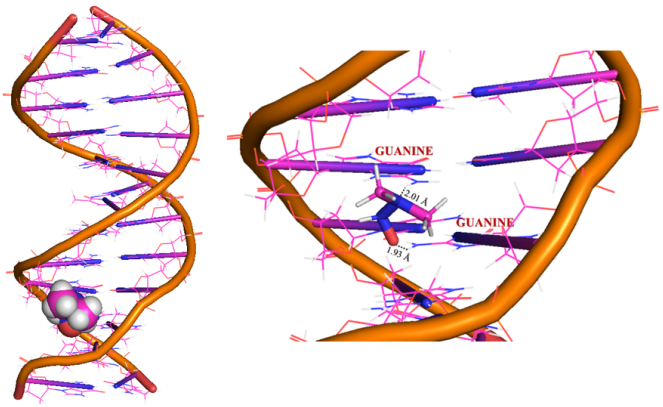

Figure 3. Snapshot pictures taken from the MD simulation, illustrating the stable equilibrium pose of the ligand NDMA in the proximity of the hDNA

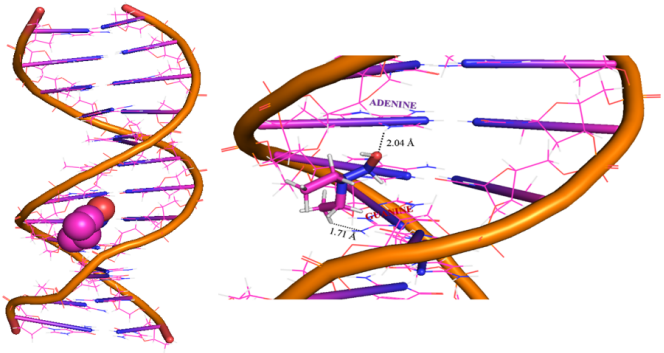

Figure 4. Snapshot pictures taken from the MD simulation, illustrating the stable equilibrium pose of the ligand NDEA in the proximity of the hDNA.

Molecular Docking Procedure

The molecular docking simulations were carried out using the AutoDock Vina 1.1.2 software program (Gaillard, 2018). A total of 400 poses were generated, with 100 poses for each simulation. As a representative of the double helix hDNA structure, 1BNA (PDB NDB ID: BDL001), which is a dodecamer of 5'-D(*CP*GP*CP*GP*AP*AP*TP*TP*CP*GP*CP*G)-3', was retrieved from the PDB database. The grid box dimensions were set to 44 × 44 × 88 $Å^3$ for blind docking. The simulations involved the NDMA and NDEA ligands and their interactions with the receptor structure of 1BNA. The simulations demonstrated the interactions and the drug's binding to the receptor. The docking scores obtained in kcal/mol represent the Gibbs free binding energy. Within all the simulations, the most accurate docking poses and favourable binding energies, identified among the best-clustered data, were selected as the initial molecule design structures and input files for the subsequent molecular dynamics (MD) simulations.

Molecular Dynamics (MD) Simulations

The input files and their corresponding chemical structures for the MD simulations were selected from the docking poses with the most favourable binding energies (Cheraghi et al., 2023; Şenel et al., 2022; Şenel et al., 2020) as shown in the scientific literature. Schrödinger's Maestro Desmond Programme (Desmond, 2017) was utilised for running the molecular dynamics (MD) simulations, each spanning 50 ns with 5000 poses at 10 ps intervals. To ensure accuracy, each MD simulation was repeated three times with varying different seed numbers, confirming the correctness of the simulation parameters and the structures of the complexes formed by the NDMA and NDEA with 1BNA. Throughout the MD simulations, the dynamic characteristics of the ligand-receptor complexes were evaluated longitudinally. A grid box measuring 110 × 110 × 110 $Å^3$ with a 0.5Å spacing was utilised to define the simulation area, allowing for comprehensive coverage during the simulation. TIP3P-type water molecules were incorporated within the grid box, and 0.15 M NaCl ions were introduced to maintain system neutrality. The simulation conditions were set to NPT at 310 K using the temperature coupling equations of Nose-Hoover (Evans & Holian, 1985), alongside a constant pressure of 1.01 bar achieved through Martyna Tobias-Klein pressure coupling (Martyna, Tobias, & Klein, 1994). The system was not constrained, and the default fitting for the OPLS 3.0 standards provided the initial velocity values for the forefield calculations. Hydrogen bonds that formed during the interaction of ligands with the 1BNA structure were investigated. The NDMA- and NDEA-bound DNA complexes were (Figure 3-4) to illustrate the interaction and binding site of the ligands on 1BNA.

RESULTS

Selectivity

The selectivity of the method against the matrix components was evaluated against a blank solvent. No peak at the retention time of the analytes was observed in the solvent chromatogram (Figure 5).

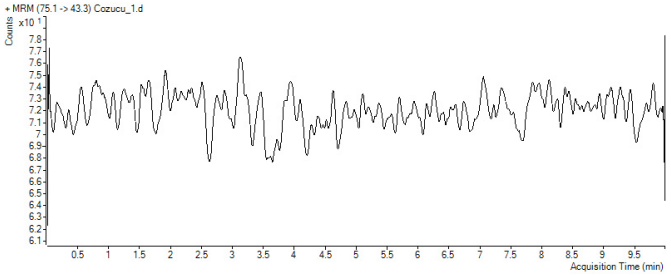

Figure 5. Blank solvent chromatogram

Carryover

During validation, the carryover was determined by the solvent injected between the calibration standards and the QC samples. There was no carryover in the injected solvent chromatogram after injecting the highest concentration level standard solution (Figure 6).

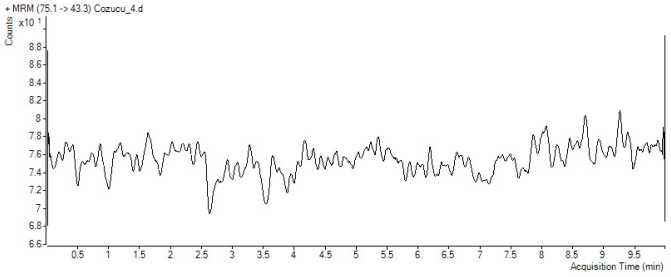

Figure 6. Blank solvent chromatogram after the highest concentration standard solution

Linearity

The linearity of the detector response at decreasing concentrations in the analytical dilutions was investigated. The calibration curves were prepared for the quantification of the samples. The calibration curves consist of 5 concentration levels including NDMA and NDEA (5, 10, 50, 100, 150 ng/mL). The correlation coefficients of the calibration curves are in the acceptable range of 0.99 for both NDMA and NDEA. The accuracy and precision results of the calibration curve concentration levels are given in Table 1-2.

Limit of detection (LOD) and limit of quantitation (LOQ)

The analyte concentrations with a signal-to-noise ratio of ≥ 3.0 and ≥ 10.0 are determined as the LOD and LOQ, respectively. The LOQ is also the initial concentration level of the calibration curve. In the LOD study, it was determined as S/N:3.24 for NDMA and S/N:13.77 for NDEA. In the LOQ study, it was determined that S/N:17.60 for NDMA and S/N:24.79 for NDEA (Figure 7).

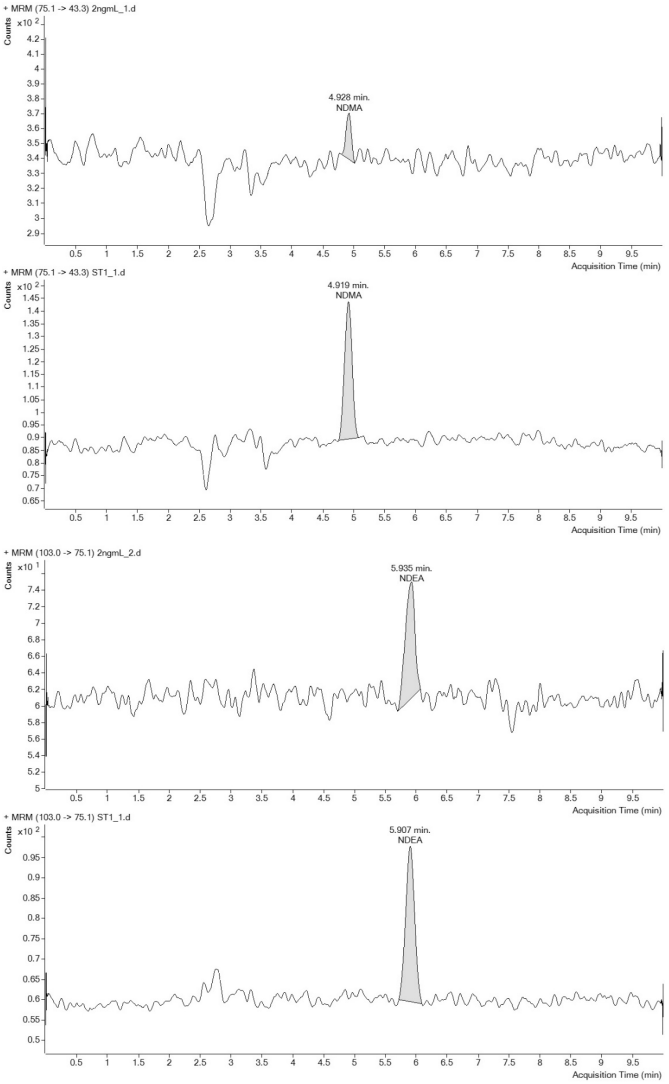

Figure 7. Chromatograms of LOD and LOQ for NDMA and NDEA

Accuracy and precision

The accuracy and the precision were calculated by analysis of low, medium, and high concentration levels of QC samples. The QC samples had 5, 75, and 150 ng/mL concentration levels. The percentage of the coefficient of variation (%CV) and the percentage of recovery were calculated for the presentation of the accuracy and the precision, respectively. A summary of the accuracy and precision is presented in Table 3-4. The results show that the method has good accuracy and precision. The intra-day and inter-day accuracy and precision values for NDMA range from 100.36 to 111.73 and from 1.68 to 5.75, respectively. For NDEA, these values range from 96.24 to 101.81 and from 0.34 to 8.77, respectively.

Table 1. Accuracy and precision results of the calibration standards for NDMA

Calibration standards (ng/mL)	Mean	Recovery %	Standard Deviation (SD)	Coefficient of variation %CV	n
5	4.84	96.73	0.42	8.59	6
10	9.98	99.78	0.68	6.86	6
50	50.29	100.59	2.92	5.81	6
100	99.73	99.73	6.09	6.11	6
150	150.07	100.05	7.74	5.16	6

Table 2. Accuracy and precision results of the calibration standards for NDEA

Calibration standards (ng/mL)	Mean	Recovery %	Standard Deviation (SD)	Coefficient of variation %CV	n
5	4.93	98.65	0.40	8.15	6
10	9.84	98.42	0.73	7.39	6
50	51.11	102.22	1.46	2.85	6
100	99.00	99.00	3.28	3.31	6
150	150.31	100.20	2.69	1.79	6

System suitability

System suitability was calculated as the theoretical plate number (N) > 2000, capacity factor (k') >, resolution (Rs) > 2, and tailing factor (T) ≤ 2 for NDMA and NDEA. Detailed parameters are given in Table 5.

Matrix Effect

The matrix effect was calculated by spiking the matrix (placebo) of a capsule drug product containing the active substance Nizatidine. The matrix effect results were 12.5% for NDMA and 11.6% for NDEA.

Molecular Docking and Molecular Dynamics Results

NDMA is a strong drug impurity and suppresses the DNA via gene silencing, as shown in Figures 3 and 8. It selectively binds onto the minor groove location and chooses solely and strictly Guanine nucleotides with a strong 9.9 kcal/mol inhibition score, Δ(ΔG) for 1BNA. It binds to two Guanine nucleotides simultaneously by forming H-bonds via its amine nitrogen and hydroxyl oxygen at distances 2.01 Å, and 1.93 Å, respectively. The drug impurity positions itself towards the minor groove region of the 1BNA and it is stabilised via the H-bonds. The suppression of 1BNA causes an alteration in the strong, rigid phosphodiester helical structure resembling a bent, distorted shape.

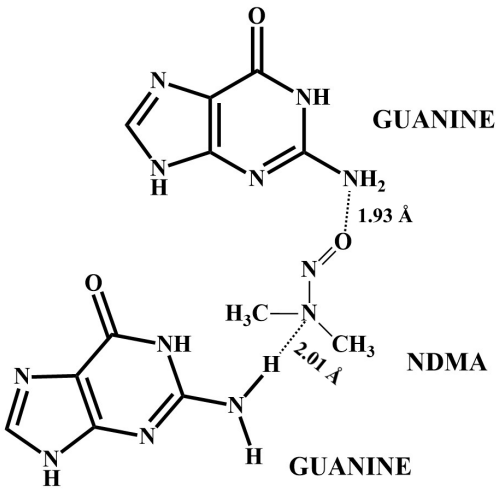

Figure 8. 2D pose of the hydrogen bonding of NDMA's functional groups to Guanine nucleic bases

NDEA is also capable of suppressing the DNA via gene

Table 3. Accuracy and precision results of the QC samples for NDMA

	Intra-day					Inter-day				
QC samples (ng/mL)	Mean	Recovery %	SD	%CV	n	Mean	Recovery %	SD	%CV	n
5	5.59	111.73	0.29	5.22	6	5.42	108.35	0.31	5.75	18
75	78.16	104.21	1.43	1.83	6	78.88	105.17	1.32	1.68	18
150	150.54	100.36	4.06	2.70	6	151.11	100.74	4.31	2.85	18

Table 4. Accuracy and precision results of the QC samples for NDEA

	Intra-day					Inter-day				
QC samples (ng/mL)	Mean	Recovery %	SD	%CV	n	Mean	Recovery %	SD	%CV	n
5	5.08	101.61	0.34	6.66	6	5.05	101.02	0.44	8.77	18
75	76.33	101.78	1.48	1.93	6	76.36	101.81	1.80	2.36	18
150	144.36	96.24	1.47	1.02	6	145.30	96.86	2.03	1.40	18

Table 5. System suitability results and acceptability limits

Parameter	Value for NDMA	Value for NDEA	Limit (FDA guideline)
Retention time (min)	4.912	5.886	-
Peak Width (W)	0.114	0.141	-
Tailing (T)	1	1.1	$T \leq 2$
Theoretical Plates (N)	9259	2220	$N > 2000$
Resolution (Rs)	48.1	23.6	$Rs > 2$
Capacity Factor (k)	490.2	587.6	$k' > 2$

silencing with nucleotide regioselectivity by coordinating itself into the minor groove domain of the hDNA in Figures 4 and 9. Its regioselectivity is equally the same for Guanine and Adenine nucleotides. The inhibition score was a bit higher than NDMA where $\Delta(\Delta G)$ value was found to be -10.3 kcal/mol for 1BNA.

Since 1BNA mimics the human DNA template in the scientific literature, its utilisation under the physiological pH of 7.4 proves us here that these two drug impurities, NDMA and NDEA, cause a DNA suppression, DNA toxicity, with the minor groove type of mode of binding and significantly efficient inhibition scores via strong Hydrogen bonds. In Figure 10, the RMSD data can be observed vindicating the MD results of Figures 3 to 4, where both NDMA and NDEA reach a much more stabilised complex structure, oscillations are much lower compared to hDNA (1-BNA dodecamer) itself. This is the evidence of the great suppressive/inhibitive nature of NDMA and NDEA towards human DNA, it forms a quite strong Hydrogen bonding after 10 ns passes in the simulation and keeps the oscillations of all the atoms of the complex under 0.5 Å.

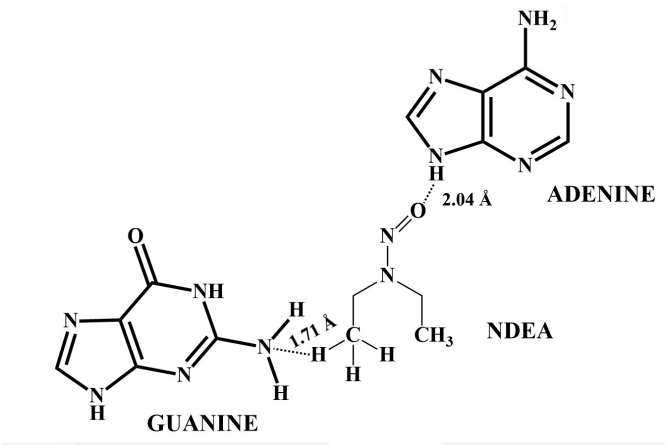

Figure 9. 2D pose of the hydrogen bonding of NDEA's functional groups to Adenine and Guanine nucleic bases

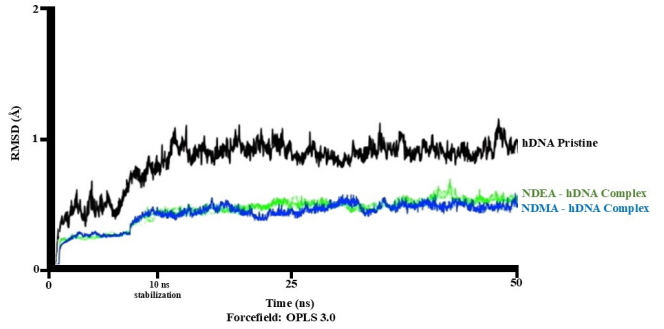

Figure 10. The root mean square deviation (RMSD) plot of the MD result is illustrated. The NDEA-hDNA complex is in green, the NDMA-hDNA complex is in blue, and the hDNA (1-BNA dodecamer) is in black colour

DISCUSSION

Nitrosamine impurities need to be limited to acceptable levels in drug products because of their highly mutagenic and carcinogenic properties. Regulatory authorities such as the FDA and EMA have published several notices to guide drug manufacturers in controlling and analysing these impurities to ensure they remain at acceptable levels. LC-MS/MS and GC-MS/MS techniques are the analytical methods used for the determination of nitrosamine impurities. A potential source of nitrosamine impıirities can enter drug substances, raw materials, reagents, catalysts, and solvents.

The non-bonded interactions are stronger due to the larger size of NDEA than NDMA. One of the hydrogen of the ethyl group approaches Guanine at a distance of 1.71 Å to form a vdW-type interaction, which is absent in NDMA. The typical H-bond occurs hydroxy oxygen of the ligand and Adenine at a distance of 2.04 Å (Figure 4). The binding mode of the drug impurity NDEA is the same as that of NDMA, but the nucleotide preference of oxygen changes to Adenine and the ligand is coordinated onto the minor groove region of the 1BNA.

CONCLUSION

LC-MS/MS is the most reliable technique for determining nitrosamine impurities in drug products. The developed method can detect NDMA and NDEA at trace levels, and it is both fast and simple. In the matrix effect studies, the extraction method yielded low matrix effect results, indicating that very low nitrosamine concentrations can also be effectively detected using the ESI ion source instead of the APCI ion source.

Since 1BNA mimics the human DNA template in the scientific literature, its utilisation under the physiological conditions as a target for the drug impurities, NDMA and NDEA enabled us to show that these small organic molecules have high-affinity scores and strongly bind to the minor groove of the hDNA via strong hydrogen bonds. It is highly probable that they may cause DNA suppression and damage DNA integrity.

Peer-review: Externally peer-reviewed.

Author Contributions: Conception/Design of Study: İ.D., S.A., M.Y., D.Ö.Ü.; Data Acquisition: İ.D., S.A., M.Y., D.Ö.Ü.; Data Analysis/Interpretation: İ.D., S.A., M.Y., D.Ö.Ü.; Drafting Manuscript: İ.D., S.A., M.Y., D.Ö.Ü.; Critical Revision of Manuscript: İ.D., S.A., M.Y., D.Ö.Ü.; Final Approval and Accountability İ.D., S.A., M.Y., D.Ö.Ü.

Conflict of Interest: The authors have no conflict of interest to declare.

Financial Disclosure: The authors declared no financial support.

ORCID IDs of the authors

İbrahim Daniş 0000-0003-4646-4129
Soykan Agar 0000-0002-9870-6882
Mine Yurtsever 0000-0001-6504-7182
Durişehvar Özer Ünal 0000-0003-0754-1240

REFERENCES

Al-Kaseem, M., Al-Assaf, Z., & Karabeet, F. (2014). A Rapid, Validated RP-HPLC Method for the Determination of Seven Volatile N-Nitrosamines in Meat. *Pharmacology Pharmacy*, 05(03), 298-308. https://doi.org/10.4236/pp.2014.53037

arnes, J. M., & Magee, P. N. (1954). Some Toxic Properties of Dimethylnitrosamine. *Occupational and Environmental Medicine, 11*(3), 167-174. https://doi.org/10.1136/oem.11.3.167

Becke, A. D. (1993). Density-functional thermochemistry. III. The role of exact exchange. *The Journal of Chemical Physics, 98*(7), 5648-5652. https://doi.org/10.1063/1.464913

Cheraghi, S., Şenel, P., Dogan Topal, B., Agar, S., Majidian, M., Yurtsever, M., . . . Ozkan, S. A. (2023). Elucidation of DNA-Eltrombopag Binding: Electrochemical, Spectroscopic and Molecular Docking Techniques. Biosensors, 13(3), 300. https://doi.org/10.3390/bios13030300

Control of nitrosamine impurities in human drugs. (2021). https://www.fda.gov/media/141720/download. (Accessed December 11, 2024).

Dennington, R., Keith, T., & Millam, J. (2009). GaussView, version 5. Desmond, D. (2017). Shaw Research: New York. In: NY.

Evans, D. J., & Holian, B. L. (1985). The nose–hoover thermostat. *The Journal of Chemical Physics, 83*(8), 4069-4074.

Frisch, M., Trucks, G., Schlegel, H., Scuseria, G., Robb, M., Cheeseman, J., . . . Petersson, G. (2009). 09, Revision D. 01, Gaussian. Inc., Wallingford, CT.

Gaillard, T. (2018). Evaluation of AutoDock and AutoDock Vina on the CASF-2013 Benchmark. *Journal of Chemical Information and Modeling, 58*(8), 1697-1706. https://doi.org/10.1021/acs.jcim.8b00312

ICH Q2 (R1). (2005). Validation of Analytical Procedures: Text and Methodology, https://database.ich.org/sites/default/files/Q2%28R1%29%20Guideline.pdf. (Accessed December 11, 2024).

Kul, A., & Sagirli, O. (2023). Elimination of matrix effects in urine for determination of ethyl glucuronide by liquid chromatography-tandem mass spectrometry. *Rapid Communications in Mass Spectrometry, 37*(23), e9643. https://doi.org/10.1002/rcm.9643

Li, W., Chen, N., Zhao, Y., Guo, W., Muhammed, N., Zhu, Y., & Huang, Z. (2018). Online coupling of tandem liquid-phase extraction with HPLC-UV for the determination of trace N-nitrosamines in food products. *Analytical Methods, 10*(15), 1733-1739. https://doi.org/10.1039/c8ay00014j

Li, Y., & Hecht, S. S. (2022). Metabolic Activation and DNA Interactions of Carcinogenic N-Nitrosamines to Which Humans Are Commonly Exposed. *International Journal of Molecular Sciences, 23*(9). https://doi.org/10.3390/ijms23094559

Lv, J., Wang, L., & Li, Y. (2017). Characterization of N-nitrosodimethylamine formation from the ozonation of ranitidine. *Journal of Environmental Sciences*, 58, 116-126. https://doi.org/10.1016/j.jes.2017.05.028

M7(R1) assessment and control of DNA reactive (mutagenic) impurities in pharmaceuticals to limit potential carcinogenic risk. (2018). https://www.fda.gov/media/85885/download. (Accessed December 11, 2024).

Magee, P. N., & Barnes, J. M. (1956). The production of malignant primary hepatic tumours in the rat by feeding dimethylnitrosamine. *British Journal of Cancer*, 10(1), 114-122. https://doi.org/10.1038/bjc.1956.15

Martyna, G. J., Tobias, D. J., & Klein, M. L. (1994). Constant pressure molecular dynamics algorithms. *The Journal of Chemical Physics, 101*(5), 4177-4189.

Masada, S., Tsuji, G., Arai, R., Uchiyama, N., Demizu, Y., Tsutsumi, T., . . . Okuda, H. (2019). Rapid and efficient high-performance liquid chromatography analysis of N-nitrosodimethylamine impurity in valsartan drug substance and its products. *Scientific Reports*, 9(1). https://doi.org/10.1038/s41598-019-48344-5

McConkey, B. J., Sobolev, V., & Edelman, M. (2002). The performance of current methods in ligand–protein docking. *Current Science, 83*(7), 845-856. Retrieved from http://www.jstor.org/stable/24107087

Nawrocki, J., & Andrzejewski, P. (2011). Nitrosamines and water. *Journal of Hazardous Materials*, 189(1), 1-18. doi:https://doi.org/10.1016/j.jhazmat.2011.02.005

Ngongang, A. D., Duy, S. V., & Sauvé, S. (2015). Analysis of nine N-nitrosamines using liquid chromatography-accurate mass high resolution-mass spectrometry on a Q-Exactive instrument. *Analytical Methods, 7*(14), 5748-5759. https://doi.org/10.1039/c4ay02967d

Nitrosamine impurities in human medicinal products. (2020). https://www.ema.europa.eu/en/human-regulatory-overview/post-authorisation/pharmacovigilance-post-authorisation/referral-procedures-human-medicines/nitrosamine-impurities. (Accessed December 11, 2024).

Ponting, D. J., Dobo, K. L., Kenyon, M. O., & Kalgutkar, A. S. (2022). Strategies for Assessing Acceptable Intakes for Novel N-Nitrosamines Derived from Active Pharmaceutical Ingredients. *Journal of Medicinal Chemistry, 65*(23), 15584-15607. https://doi.org/10.1021/acs.jmedchem.2c01498

Preussmann, R. (1984). Carcinogenic N-nitroso compounds and their environmental significance. *Naturwissenschaften, 71*(1), 25-30. https://doi.org/10.1007/bf00365976

Roux, J. L., Gallard, H., Croué, J.-P., Papot, S., & Deborde, M. (2012). NDMA Formation by Chloramination of Ranitidine: Kinetics and Mechanism. *Environmental Science & Technology, 46*(20), 11095-11103. https://doi.org/10.1021/es3023094

cherf-Clavel, O., Kinzig, M., Besa, A., Schreiber, A., Bidmon, C., Abdel-Tawab, M., . . . Holzgrabe, U. (2019). The contamination of valsartan and other sartans, Part 2: Untargeted screening reveals contamination with amides additionally to known nitrosamine impurities. *Journal of Pharmaceutical and Biomedical Analysis*, 172, 278-284. https://doi.org/10.1016/j.jpba.2019.04.035

Sedlo, I., Kolonić, T., & Tomić, S. (2021). Presence of nitrosamine impurities in medicinal products. *Archives of Industrial Hygiene and Toxicology, 72*(1), 1-5. https://doi.org/10.2478/aiht-2021-72-3491

Haikh, T., Gosar, A., & Sayyed, H. (2020). Nitrosamine Impurities in Drug Substances and Drug Products. 2, 48-57. https://doi.org/10.5281/zenodo.3629095

Şenel, P., Agar, S., İş, Y. S., Altay, F., Gölcü, A., & Yurtsever, M. (2022). Deciphering the mechanism and binding interactions of Pemetrexed with dsDNA with DNA-targeted chemotherapeutics via spectroscopic, analytical, and simulation studies. *Journal of Pharmaceutical and Biomedical Analysis*, 209, 114490. https://doi.org/10.1016/j.jpba.2021.114490

Şenel, P., Agar, S., Sayin, V. O., Altay, F., Yurtsever, M., & Gölcü, A. (2020). Elucidation of binding interactions and mechanism of Fludarabine with dsDNA via multispectroscopic and molecular docking studies. *Journal of Pharmaceutical and Biomedical Analysis*, 179, 112994. https://doi.org/10.1016/j.jpba.2019.112994

Thresher, A., Foster, R., Ponting, D. J., Stalford, S. A., Tennant, R. E., & Thomas, R. (2020). Are all nitrosamines concerning? A review of mutagenicity and carcinogenicity data. *Regulatory Toxicology and Pharmacology*, 116, 104749. https://doi.org/10.1016/j.yrtph.2020.104749

Zhao, Y. Y., Boyd, J., Hrudey, S. E., & Li, X. F. (2006). Characterization of New Nitrosamines in Drinking Water Using Liquid Chromatography Tandem Mass Spectrometry. *Environmental Science & Technology, 40*(24), 7636-7641. https://doi.org/10.1021/es061332s

How cite this article

Daniş, İ., Agar, S., Yurtsever, M., Özer Ünal, D. (2024). High Performance Liquid Chromatography-Tandem Mass Spectrometric determination of carcinogen nitrosamine impurities from pharmaceuticals and DNA binding confirmation aided by molecular docking application. *İstanbul Journal of Pharmacy, 54*(3): 386–394. DOI: 10.26650/IstanbulJPharm.2024.1500047